JACS
JOURNAL OF THE AMERICAN CHEMICAL SOCIETY

Article

pubs.acs.org/JACS

Incorporation and Controlled Release of Silyl Ether Prodrugs from PRINT Nanoparticles

Matthew C. Parrott,[†,§,#] Mathew Finniss,[†,§,#] J. Chris Luft,[†,§,#] Ashish Pandya,[†,§,#] Anuradha Gullapalli,[†,§,#] Mary E. Napier,[†,§,#,⊗] and Joseph M. DeSimone*[,†,‡,§,∥,⊥,#,¶,○]

[†]Department of Chemistry, [‡]Department of Pharmacology, [§]Carolina Center of Cancer Nanotechnology Excellence, [∥]Institute for Advanced Materials, [⊥]Institute for Nanomedicine, [#]Lineberger Comprehensive Cancer Center, [⊗]Department of Biochemistry and Biophysics, University of North Carolina, Chapel Hill, North Carolina 27599, United States

[¶]Department of Chemical and Biomolecular Engineering, North Carolina State University, Raleigh, North Carolina 27695, United States

[○]Sloan-Kettering Institute for Cancer Research, Memorial Sloan-Kettering Cancer Center New York, New York 10021, United States

Supporting Information

ABSTRACT: Asymmetric bifunctional silyl ether (ABS) prodrugs of chemotherapeutics were synthesized and incorporated within 200 nm × 200 nm particles. ABS prodrugs of gemcitabine were selected as model compounds because of the difficulty to encapsulate a water-soluble drug within a hydrogel. The resulting drug delivery systems were degraded under acidic conditions and were found to release only the parent or active drug. Furthermore, changing the steric bulk of the alkyl substituents on the silicon atom could regulate the rate of drug release and, therefore, the intracellular toxicity of the gemcitabine-loaded particles. This yielded a family of novel nanoparticles that could be tuned to release drug over the course of hours, days, or months.

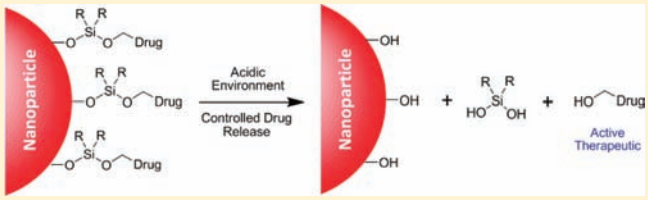

INTRODUCTION

Prodrugs are considered inactive molecules prior to administration, but after exposure to certain physiological conditions, they are triggered to metabolize or spontaneously breakdown into an active therapeutic.[1] Common physiological conditions used to degrade prodrugs include acidic milieus, reducing environments and elevated enzymatic levels.[2−4] Frequently, the acidic conditions known to exist in the endocytic pathway in cancer cells[5] in areas of inflammation[6] and within tumor tissue[7] are exploited to catalyze the degradation of prodrugs. Consequently, a high payload of drug can be deposited in these areas thereby increasing drug efficacy, reducing non-specific uptake by healthy tissue, and increasing patient compliance. Previously, acid sensitive prodrugs have been assembled using a number of specialized chemistries including hydrazone,[8] trityls,[9] aconityls,[10] vinyl ethers,[11] poly(ketals),[12,13] acetals,[14] poly(ortho esters),[15] and thiopropionates,[16] but these strategies lack tunability, produce toxic byproducts, or necessitate exhaustive multistep syntheses.

Silyl ethers are among the most widely used protecting groups for the alcohol functionally because the rate of deprotection can be modulated by simply altering the substituents on the silicon atom. As a result, the synthesis of small-molecule silyl ether prodrugs (Figure 1a) have been explored using a variety of acid sensitive silane attachments including trimethyl silyl ether (TMS), triethyl silyl ether (TES), and triisopropyl silyl ether (TIPS). Although these materials are

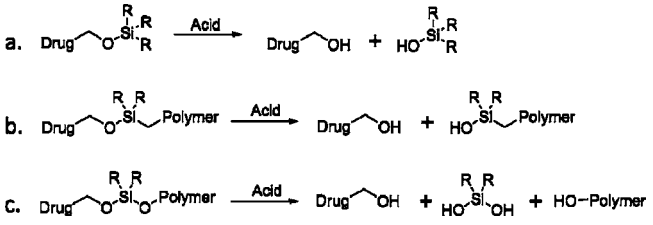

Figure 1. Three types of silyl ether prodrugs: (a) small molecule monofunctional silyl ether, (b) polymeric monofunctional silyl ether prodrug, and (c) polymeric asymmetric bifunctional silyl ether prodrug.

labile in vivo, they are typically fastidious because of their vulnerability to acidic workups.[17] This limitation can be alleviated by incorporating silyl ether prodrugs within a polymeric drug delivery system. The combination of a small molecule drug with high molecular weight polymer provides protection for the therapeutic, and reduces the rate of degradation. Previously, polybutadiene and polyamine polymers have been functionalized with monofunctional silyl ether prodrugs (Figure 1b) of antiulcer prostaglandins,[18,19] which were designed to degrade under the harsh acidic environment found in the stomach. Although these materials were acid sensitive and the therapeutic was released in a controlled

Received: March 9, 2012
Published: April 23, 2012

   dx.doi.org/10.1021/ja301710z | J. Am. Chem. Soc. 2012, 134, 7978−7982

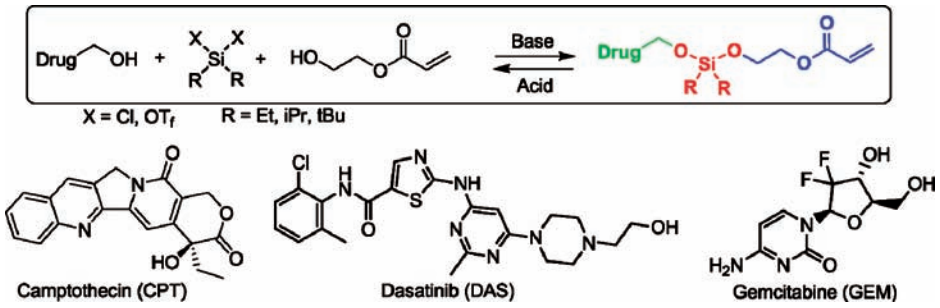

Figure 2. Asymmetric bifunctional silyl ether (ABS) prodrugs of camptothecin, dasatinib, and gemcitabine. Each ABS prodrug is composed of three parts: (1) a chemotherapeutic (green), (2) a silyl ether linkage (red), and (3) a polymerizable monomer for particle incorporation (blue).

fashion, the starting polymer and polymer byproduct generated after degradation were not water-soluble, biodegradable, or biocompatible. Furthermore, the reaction between the small molecule drug and the chlorosilane-decorated polymer gave incomplete conversion resulting in low drug loading.

To mitigate these drawbacks, we have exploited the sensitivity and tunability of bifunctional silyl ether linkers that are composed of a C−O−Si−O−C bond arrangement (Figure 1c). The implementation of an ether linkage on each side of the silicon atom allows for the acid sensitive product to revert back to its original, unmodified starting material. This ensures that the therapeutic will be released in its active form, and that the liberated biocompatible polymer will be safe in the body after degradation. Previously, we employed bifunctional silyl ether chemistry to fabricate microparticles that could be internalized within cells and degrade under intracellular conditions.[29] These microparticles showed little to no toxicity because the silane byproducts were innocuous and the remaining polymer, poly(hydroxy ethyl acrylate), was water-soluble and biocompatible. Understanding the versatility of bifunctional silyl ether chemistry, we set out to design a novel silyl ether prodrug that could be incorporated within a nanoparticle carrier. Following exposure to the acid environment found in cancer cells and tumors, the nanoparticle would be triggered to release a high payload of drug within the diseased site. Furthermore, changing the substituents on the silicon atom would allow for controlled and tunable drug-release. The integration of silyl ether prodrugs within a nanoparticle would, therefore, provide a nanodevice that could be engineered to release a drug specifically at the site of disease and at a programmed rate thereby minimizing toxic side effects.

■ RESULTS AND DISCUSSION

Herein, and for the first time, we report how to incorporate a water-soluble, clinically relevant drug into a state-of-the-art nanoparticle platform using bifunctional silyl ether chemistry. The bifunctional silyl ether functionality was selected as an ideal prodrug linkage for four reasons: (1) silyl ethers are typically acid sensitive and are known to degrade under acidic conditions found in the body; (2) changing the substituents on the silicon atom allows for the rate of drug release to be modulated or tuned; (3) nontoxic, commercially available monomers or polymers are amenable with silyl ether chemistry and provide the necessary functionality for the incorporation within nanoparticles; and (4) upon degradation, there is no trace of the silyl ether modification on the drug. Furthermore, the synthesis requires only one step and minimal workup. For these reasons, we believe that silyl ether prodrugs are far superior to conventional prodrugs.

To show the versatility of silyl ether chemistry, we selected three chemotherapeutics for their pendant alcohol functionality. Specifically, camptothecin (CPT), dasatinib (DAS), and gemcitabine (GEM) were identified as molecules that would be amenable with silyl ether chemistry. Each prodrug was synthesized as a polymerizable monomer, which allowed for facile incorporation and high drug loading within a nanoparticle. The modification occurred by reacting a dichlorodialkyl silane (Et, iPr,) or di-*t*-butylsilyl ditriflate with the pendant alcohol on the chemotherapeutic. Each conversion was monitored by thin layer chromatography (TLC), and upon complete consumption of the starting material, hydroxyl ethyl acrylate (HEA) was added. The resulting molecule was synthesized in one step and was composed of three parts: a chemotherapeutic, an acid sensitive bifunctional silyl ether linkage, and a polymerizable monomer for particle fabrication (Figure 2).

We have elected to call this new class of prodrug an asymmetric bifunctional silyl ether (ABS). From the three model chemotherapeutics, gemcitabine was selected as an ideal candidate for the incorporation within nanoparticles because of it is high water solubility and, hence, its difficulty at being retained within a hydrogel particle for any significant period of time. Typically, hydrophobic drugs are trapped within hydrophobic nanoparticles[20] or within hydrophobic cores of nanoparticles.[21−23] Limited research has been conducted on incorporating water-soluble drugs within nanoparticles. This is likely due to the significant loss of the cargo through diffusion or burst release once the particle is placed in an aqueous environment. The incorporation of an ABS prodrug of gemcitabine within a nanoparticle would therefore be useful and would confirm the versatility of the bifunctional silyl ether linkage.

Three ABS prodrugs of gemcitabine, where the R groups were ethyl, isopropyl, or *tert*-butyl, were separately incorporated into "Trojan Horse" nanoparticles using a particle fabrication technique called particle replication in nonwetting templates (PRINT).[24] PRINT is a top-down technique used to synthesize microparticles[25,26] and nanoparticles[27,28] with well-defined shape and size. Cylindrical nanoparticles with dimensions of 200 nm × 200 nm were fabricated (Figure 3) with 20 wt % of the ABS prodrug, and the remaining bulk of the particle comprised a cross-linker (PEG1000diacrylate), a positively charged agent to facilitate cellular internalization (aminoethyl methacrylate-hydrochloride), a fluorescent dye (fluorescein *o*-acrylate), and a photoinitiator (1-hydroxycyclohexyl phenyl ketone). This particle composition was selected for its ability to rapidly internalize within acidic cellular compartments. Detailed microscopy and internalization of this composition has been

dx.doi.org/10.1021/ja301710z | J. Am. Chem. Soc. 2012, 134, 7978−7982

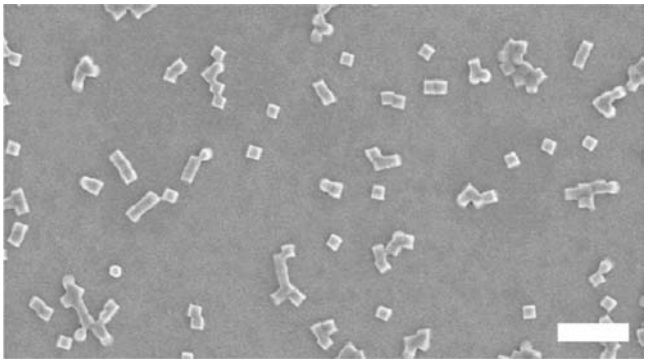

Figure 3. Scanning electron micrograph of 200 nm × 200 nm PRINT particles containing gemcitabine (scale bar = 1 μm).

shown elsewhere.[27] Moreover, the degradation of this composition containing different bifunctional silyl ether cross-linkers has been found to be nontoxic in multiple in vitro assays.[29] For this study, a high degree of cross-linking was implemented to facilitate slow and controlled release of the gemcitabine cargo. Each particle fabricated with a gemcitabine ABS prodrug had a particle size range of 299 ± 6.46 nm and a ζ potential of +22.5 ± 3.53 mV.

A quantitative analysis of gemcitabine release was performed on particles fabricated with diethyl gemcitabine ABS prodrug (Et-GEM), diisopropyl gemcitabine ABS prodrug (iPr-GEM), and di-*tert*-butyl gemcitabine ABS prodrug (tBu-GEM). The particles were degraded in solutions buffered at pH 5.0 and pH 7.4 to mimic intracellular and physiological conditions, respectively. The release experiment was maintained at 37 °C and continued until the particles no longer released gemcitabine. Aliquots of the solution were removed and filtered, and the supernatant was analyzed by high-performance liquid chromatography and compared against the maximum theoretical loading to determine percent release and encapsulation efficiency. Chromatograms taken at different time points over 1 day indicated controlled release of gemcitabine from PRINT particles fabricated with the Et-GEM prodrug (Figure 4). Moreover, the gemcitabine released

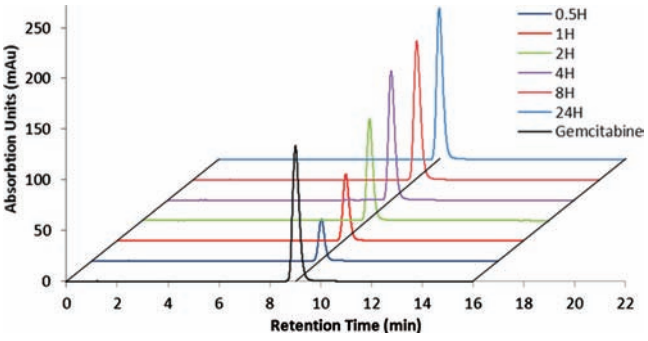

Figure 4. Chromatograms of the unmodified gemcitabine (black) and gemcitabine released from nanoparticles fabricated with diethyl gemcitabine ABS prodrug over 24 h.

from the PRINT particles had the same retention time (~9.0 min) as the unmodified gemcitabine, demonstrating that only the active form of the drug was being released from the particles.

A plot of gemcitabine release versus time for each particle can be seen in Figure 5. It was apparent that, as the steric bulk

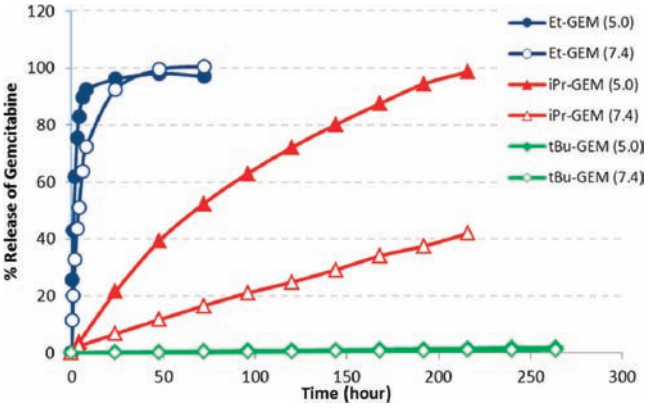

Figure 5. Percent release of gemcitabine versus time for 200 nm × 200 nm PRINT nanoparticles fabricated with Et-GEM (blue), iPr-GEM (red), and tBu-GEM (green) prodrugs. Closed symbols represent particles degraded at pH 5.0 and open symbols represent particles degraded at pH 7.4.

around the silicon atom increased, the rate of drug release decreased. For example, particles degraded at pH 5.0 had a half-life of release ($t_{1/2}$) of 1.36 h for Et-GEM, 68.5 h for iPr-GEM, and 6995 h for tBu-GEM (Table 1). Particles degraded under

Table 1. Release Half-Lives ($t_{1/2}$) and Relative Rates of Release from 200 nm × 200 nm PRINT Particles

	ethyl-GEM		isopropyl-GEM		*t*-butyl-GEM	
pH	5.0[a]	7.4[a]	5.0[a]	7.4[a]	5.0[b]	7.4[b]
$t_{1/2}$ (h)	1.36	3.91	68.5	274	6995	13055
Rel. rate	1	2.88	50.4	201	5143	9599

[a]Data fit to an exponential growth (R^2 > 0.99). [b]Extrapolated from a linear fit (R^2 > 0.99).

physiological conditions (pH 7.4) showed a significantly slower rate of release. Encapsulation efficiency of the gemcitabine within the nanoparticle was determined by comparing the final concentration of released gemcitabine against the theoretical loading of the ABS prodrug. For the particles fabricated with Et-GEM and iPr-GEM, the amount of gemcitabine released was >95% of the theoretical maximum, indicating near-quantitative encapsulation of the drug within the nanoparticle.

To test the practicality of these nanoparticles under physiological conditions, cell viability experiments were used to determine half maximal inhibitory concentrations (IC_{50}) of each gemcitabine ABS particle. This was accomplished by separately dosing a wide concentration range of all three particle types (Et-GEM, iPr-GEM, and tBu-GEM) onto LNCaP cells and comparing the cell viability against unmodified gemcitabine, and against blank particles without drug. The cytotoxicity of each particle was determined using a CellTiter-Glo luminescent cell viability assay after a 72 h incubation time (Figure 6). Remarkably, the particles loaded with 20 wt % of the tBu-GEM prodrug showed the same cell viability as the blank particles, thereby completely halting the toxic nature of the gemcitabine on LNCaP cells. This illustrates the high stability of the *tert*-butyl silyl ether linkage and its ability to render the nanoparticle completely nontoxic even at extremely high drug concentrations. The release of the drug from the nanoparticles could be modulated by simply changing the steric bulk around the silyl ether leading to different effective toxicities. Utilizing iPr-GEM and Et-GEM particles, their

dx.doi.org/10.1021/ja301710z | J. Am. Chem. Soc. 2012, 134, 7978–7982

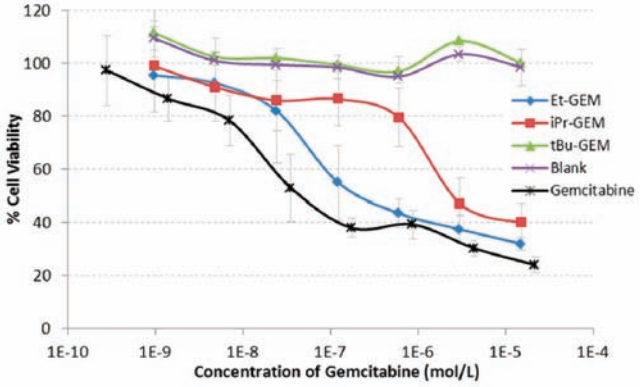

Figure 6. Cell viability assay (CellTiter-Glo) of 200 nm × 200 nm particles fabricated from Et-GEM (blue), iPr-GEM (red), and tBu-GEM (green) prodrugs versus blank particles (purple) and free gemcitabine (black). The assay was performed using LnCAP cells.

respective IC_{50} values were measured to be 2791 and 154 nM, with the latter being almost as toxic as the unmodified gemcitabine. When compared to unmodified gemcitabine, particles fabricated with Et-GEM, iPr-GEM, and tBu-GEM prodrugs were 3.5, 64.3, and infinitely less toxic, respectively (Table 2). We attribute this decrease in toxicity to the time

Table 2. IC_{50} values of gemcitabine containing nanoparticles on LNCaP Cells, and Relative Cellular Response

	free GEM	Et-GEM	iPr-GEM	tBu-GEM	blank
IC_{50} (nM)	43.4	154	2791	-	-
Rel. Response	1.0	3.5	64.3	∞	∞

[a]Data fit to an exponential decay (R^2 > 0.99).

required for a particle to internalize within a cell and the time required to degrade the silyl ether linkage under intracellular conditions.

To visualize the effect of internalized ABS nanoparticles on cells, the particles were dosed onto LNCaP cells and monitored using a PathScan apoptosis and proliferation multiplex IF kit. This method allowed us to simultaneously monitor mitotic index and programmed cell death using laser scanning confocal microscopy (Figure 7). The PathScan kit contains a mixture of three primary antibodies targeted against α-tubulin, phosphor-histone H3 (Ser10), and cleaved −PARP (Asp214). The presence of α-tubulin (red in confocal) indicates a healthy cell containing fundamental cytosolic fibers important in meiotic/mitotic chromosome alignment. The presence of phosphor-histone H3 (green in confocal) also indicates a healthy cell undergoing microtubule assembly during mitosis. Finally, cleaved −PARP (nucleus appears purple in confocal) is indicative of cytoskeleton proteins and nuclear protein experiencing an apoptotic event. As a consequence of the high toxicity of gemcitabine on LNCaP cells, it was extremely difficult to find and image cells dosed with free gemcitabine or dosed with Et-GEM particles. The small number of remaining cells showed a deep purple nucleus and limited α-tubulin indicating the onset of apoptosis. Conversely, cells dosed with blank particles or with tBu-GEM particles showed healthy α-tubulin fibers, and in both cases, mitotic events were clearly visible in green. This further confirms the similar toxicity of Et-GEM particles to free gemcitabine. Moreover, this experiment validates the tunability of a silyl ether linkage from highly labile

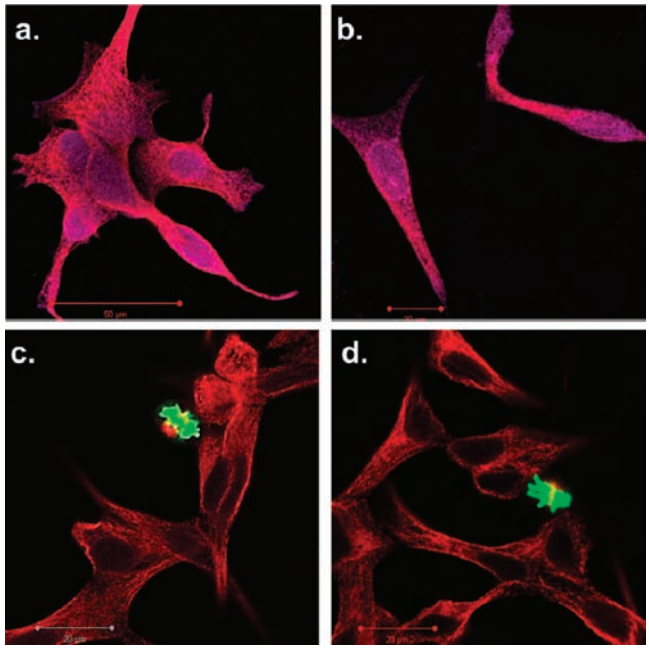

Figure 7. Confocal microscopy images of LNCaP cells stained with PathScan apoptosis and proliferation kit. The cell were separately dosed with (a) free gemcitabine, (b) Et-GEM particles, (c) tBu-GEM particles, and (d) blank particles. Red indicates a healthy cell containing fundamental cytosolic fibers important in meiotic/mitotic chromosome alignment. Green indicates a healthy cell undergoing microtubule assembly during mitosis. Purple indicates cytoskeleton proteins and nuclear protein experiencing an apoptotic event.

and toxic Et-GEM ABS to exceedingly stabile and nontoxic tBu-GEM ABS.

■ CONCLUSION

Asymmetric bifunctional silyl ether prodrugs were synthesized and analyzed as potential materials for controlled drug delivery in nanoparticles. With one simple step, we were able to synthesize a host of potential prodrugs from camptothecin, dasatinib, and gemcitabine. The ABS prodrugs of gemcitabine were incorporated into 200 nm × 200 nm PRINT nanoparticles and showed controlled and tunable release of gemcitabine. The rate of release increased as the steric bulk of the substituent on the silicon atom decreased. HPLC analysis confirmed that subsequent to silyl ether degradation, the prodrug reverted back to the original active form without any residual modification. Furthermore, release of the drug was accelerated by exposure to acidic conditions similar to those found in the cellular endocytic cycle. Detailed cellular in vitro experiments demonstrated that a particle could be fabricated to release drug rapidly and with comparable toxicities to the free drug. Particles could also be fabricated to release drug remarkably slow with minimal toxicity regardless of drug loading. Additional exploration into ABS prodrugs could lead to the development of nanoparticles with the ability of releasing drugs specifically at the diseased site in a controlled fashion. This type of treatment would be capable of treating a real world problem like cancer, while simultaneously reducing the side effects associated with conventional therapy.

dx.doi.org/10.1021/ja301710z | J. Am. Chem. Soc. 2012, 134, 7978−7982

■ ASSOCIATED CONTENT

Supporting Information

Full experimental details and characterization for all compounds. This material is available free of charge via the Internet at http://pubs.acs.org.

■ AUTHOR INFORMATION

Corresponding Author

desimone@email.unc.edu

Notes

The authors declare the following competing financial interest(s): The research reported in this paper received partial financial support from a venture capital-backed company that Prof. Joseph M. DeSimone cofounded, Liquidia Technologies (www.liquidia.com). Currently he is on the board of directors and has personal financial interests in Liquidia Technologies.

■ ACKNOWLEDGMENTS

The research was supported by the following; National Institutes of Health Grants 1R01EB009565-02, U54CA119373, and U54CA151652 (the Carolina Center of Cancer Nanotechnology), 1DP10D006432-01 (NIH Pioneer Award), the University Cancer Research Fund at the University of North Carolina at Chapel Hill, the William R. Kenan Professorship at the University of North Carolina at Chapel Hill, and a sponsored research agreement with Liquidia Technologies. We would also like to acknowledge Dr. Sohrab Habibi for obtaining the high-resolution mass spectrometry data and Dr. Marc ter Horst for helping identify the different isomers of the gemcitabine prodrugs by NMR.

■ REFERENCES

(1) Huttunen, K. M.; Raunio, H.; Rautio, J. *Pharmacol. Rev.* **2011**, *63*, 750−771.

(2) Bildstein, L.; Dubernet, C.; Couvreur, P. *Adv. Drug Delivery Rev.* **2011**, *63*, 3−23.

(3) Kratz, F.; Müller, I. A.; Ryppa, C.; Warnecke, A. *ChemMedChem* **2008**, *3*, 20−53.

(4) Rautio, J.; Kumpulainen, H.; Heimbach, T.; Oliyai, R.; Oh, D.; Jarvinen, T.; Savolainen, J. *Nat. Rev. Drug Discovery* **2008**, *7*, 255−270.

(5) Mellman, I.; Fuchs, R.; Helenius, A. *Annu. Rev. Biochem.* **1986**, *55*, 663−700.

(6) Gallin, J. I.; Goldstein, I. M.; Snyderman, R. E. *Inflammation—Basic Principles and Clinical Correlates*, 3rd ed.; Lippincott Williams & Wilkins: Philadelphia, PA, 1999.

(7) Engin, K.; Leeper, D. B.; Cater, J. R.; Thistlethwaite, A. J.; Tupchong, L.; McFarlane, J. D. *Int. J. Hyperthermia* **1995**, *11*, 211−216.

(8) Di Stefano, G.; Lanza, M.; Kratz, F.; Merina, L.; Fiume, L. *Eur. J. Pharm. Sci.* **2004**, *23*, 393−397.

(9) Patel, V. F.; Hardin, J. N.; Mastro, J. M.; Law, K. L.; Zimmermann, J. L.; Ehlhardt, W. J.; Woodland, J. M.; Starling, J. J. *Bioconjugate Chem.* **1996**, *7*, 497−510.

(10) Shen, W. C.; Ryser, H. J. P. *Biochem. Biophys. Res. Commun.* **1981**, *102*, 1048−1054.

(11) Shin, J.; Shum, P.; Thompson, D. H. *J. Controlled Release* **2003**, *91*, 187−200.

(12) Heffernan, M. J.; Murthy, N. *Bioconjugate Chem.* **2005**, *16*, 1340−1342.

(13) Sankaranarayanan, J.; Mahmoud, E. A.; Kim, G.; Morachis, J. M.; Almutairi, A. *ACS Nano* **2010**, *4*, 5930−5936.

(14) Gillies, E. R.; Frechet, J. M. J. *Bioconjugate Chem.* **2005**, *16*, 361−368.

(15) Toncheva, V.; Schacht, E.; Ng, S. Y.; Barr, J.; Heller, J. *J. Drug Targeting* **2003**, *11*, 345−353.

(16) Oishi, M.; Nagasaki, Y.; Itaka, K.; Nishiyama, N.; Kataoka, K. *J. Am. Chem. Soc.* **2005**, *127*, 1624−1625.

(17) Wuts, P. G. M.; Greene, T. W. *Greene's Protective Groups in Organic Synthesis*; 4th ed.; Wiley: New York, 2007.

(18) Perkins, W. E.; Bianchi, R. G.; Tremont, S. J.; Collins, P. W.; Casler, J. J.; Fenton, R. L.; Wagner, G. M.; McGrath, M. P.; Stolzenbach, J. C.; Kowalski, D. L.; Gasiecki, A. F.; Forester, D.; Jones, P. H. *J. Pharmacol. Exp. Ther.* **1994**, *269*, 151−156.

(19) Tremont, S. J.; Collins, P. W.; Perkins, W. E.; Fenton, R. L.; Forster, D.; McGrath, M. P.; Wagner, G. M.; Gasiecki, A. F.; Bianchi, R. G.; Casler, J. J.; Ponte, C. M.; Stolzenbach, J. C.; Jones, P. H.; Gard, J. K.; Wise, W. B. *J. Med. Chem.* **1993**, *36*, 3087−3097.

(20) Davis, M. E.; Chen, Z.; Shin, D. M. *Nat. Rev. Drug Discovery* **2008**, *7*, 771−782.

(21) Dong, X.; Mattingly, C. A.; Tseng, M. T.; Cho, M. J.; Liu, Y.; Adams, V. R.; Mumper, R. J. *Cancer Res.* **2009**, *69*, 3918−3926.

(22) Lin, L. Y.; Lee, N. S.; Zhu, J.; NystrÃ¶m, A. M.; Pochan, D. J.; Dorshow, R. B.; Wooley, K. L. *J. Controlled Release* **2011**, *152*, 37−48.

(23) Wang, A. Z.; Langer, R. S.; Farokhzad, O. C. *Annu. Rev. Med.* **2012**, *63*, 185−198.

(24) Rolland, J. P.; Maynor, B. W.; Euliss, L. E.; Exner, A. E.; Denison, G. M.; DeSimone, J. M. *J. Am. Chem. Soc.* **2005**, *127*, 10096−10100.

(25) Herlihy, K. P.; Nunes, J.; DeSimone, J. M. *Langmuir* **2008**, *24*, 8421−8426.

(26) Nunes, J.; Herlihy, K. P.; Mair, L.; Superfine, R.; DeSimone, J. M. *Nano Lett.* **2010**, *10*, 1113−1119.

(27) Gratton, S. E. A.; Ropp, P. A.; Pohlhaus, P. D.; Luft, J. C.; Madden, V. J.; Napier, M. E.; DeSimone, J. M. *Proc. Natl. Acad. Sci. U.S.A.* **2008**, *105*, 11613−11618.

(28) Petros, R. A.; Ropp, P. A.; DeSimone, J. M. *J. Am. Chem. Soc.* **2008**, *130*, 5008−5009.

(29) Parrott, M. C.; Luft, J. C.; Byrne, D. B.; Fain, J. H.; Napier, M. E.; DeSimone, J. M. *J. Am. Chem. Soc.* **2010**, *132*, 17928−17932.